

Published in final edited form as:

Biochemistry. 2005 December 20; 44(50): 16729–16736. doi:10.1021/bi0511585.

## Spectroscopic and Biochemical Characterization of Heme Binding to Yeast Dap1p and Mouse PGRMC1p<sup>+</sup>

Kaushik Ghosh<sup>&,%</sup>, Alisha M. Thompson<sup>&,%</sup>, Eric Oh<sup>\$</sup>, Xiaoli Shi<sup>#</sup>, Robert A. Goldbeck<sup>&</sup>, Zhu Zhiwu<sup>#</sup>, Chris Vulpe<sup>\$</sup>, and Theodore R. Holman<sup>&\*</sup>

<sup>&</sup>Department of Chemistry and Biochemistry, University of California, Santa Cruz, CA, 95064, USA.

<sup>#</sup>Department of Environmental Toxicology, University of California, Santa Cruz, CA, 95064, USA.

<sup>\$</sup>Department of Nutritional Sciences and Toxicology, University of California, Berkeley, CA, 94044, USA.

### Abstract

Yeast damage associated response protein (Dap1p) and mouse progesterone receptor membrane component-1 protein (mPGRMC1p) belong to a highly conserved class of putative membrane-associated progesterone binding proteins (MAPR), with Dap1p and inner zone antigen (IZA), the rat homologue of mPGRMC1p, recently being reported to bind heme. While primary structure analysis reveals similarities to the cytochrome *b*<sub>5</sub> motif, neither of the two axial histidines responsible for ligation to the heme are present in any of the MAPR proteins. In the current paper, EPR, MCD, CD, UV-vis and general biochemical methods have been used to characterize the nature of heme binding in both Dap1p and a His-tagged, membrane anchor-truncated mPGRMC1p. As isolated, Dap1p is a tetramer which can be converted to a dimer upon addition of 150 mM salt. The heme is non-covalently attached, with a maximal, *in vitro*, heme loading of approximately 30%, for both proteins. CD and fluorescence spectroscopies indicate a well ordered structure, suggesting the low heme loading is probably not due to improperly folded protein. EPR confirmed a five coordinate, high-spin, ferric resting state for both proteins, indicating one axial amino acid ligand, in contrast to the six coordinate, low-spin, ferric state of cytochrome *b*<sub>5</sub>. The MCD spectrum confirmed this conclusion for Dap1p and indicated the axial ligand is most likely a tyrosine and not a histidine, nor a cysteine, however an aspartic acid residue could not be conclusively ruled out. Potential axial ligands, which are conserved in all MAPR's, were mutated (Y78F, D118A and Y138F) and purified to homogeneity. The mutants Y78F and D118A were found to bind heme, however, Y138F did not. This result is consistent with the MCD data and indicates that Tyr138 is most likely the axial ligand to the heme in Dap1p.

Dap1p (damage associated response protein) from *S. cerevisiae* has emerged as a critical protein in sterol synthesis. Deletion of Dap1p from the genome makes yeast more sensitive to the methylating agent, methyl methanesulfonate (MMS) (1,2). MMS is widely used in yeast for mutagenesis and damage repair studies (3) because it causes various types of genomic instability (4,5). The sensitivity of *dap1Δ* is believed to be due to a lowered activity of the yeast lanosterol demethylase, Erg11p/Cyp51p, because the mutant cells were found to accumulate the ergosterol precursor intermediates, squalene and lanosterol (2). A more recent study found that the *dap1Δ* had a much lower Erg11p level than wild type, even though the *ERG11* mRNA levels were similar between the *dap1Δ* and wild type, suggesting that Dap1p is important for

<sup>+</sup>This research has been supported by NIH grant GM56062-06 (T.R.H.), Roche Foundation for Anemia Research (C.V.) and the NIH instrument grant DBI-0217922 (EPR).

\*To whom the correspondence should be sent. Phone: (831) 459-5884; Fax: (831) 459-2935; tholman@chemistry.ucsc.edu.

<sup>%</sup>These authors contributed equally to this publication.

Erg11p stability (6). Consistent with this idea, the MMS sensitivity in *dap1Δ* cells was suppressed by the overexpression of *ERG11*, or by the addition of exogenous heme (6). In addition, our lab has found that *dap1Δ* has a severe growth defect under low iron conditions (7). Based on the above data, Dap1p may function in a heme-dependent manner by controlling Erg11p stability whose activity as a P450 enzyme is known to be dependent on a prosthetic heme co-factor.

Dap1p is predicted to be a 17-kDa protein containing a heme domain which is highly homologous to the heme binding domain of cytochrome *b<sub>5</sub>* and is a member of a highly conserved family of proteins present in all eukaryotes (6,8). This family of proteins was given the name membrane-associated progesterone receptor binding proteins (MAPRs) based on the observation that a porcine member of the MAPR family bound progesterone (9). Other members of the MAPR family of proteins include inner zone antigen (IZA, also known as 25-Dx (10), VEMA (11) and Ratp28 (12)), found in the zona fasciculata of the rat adrenal cortex (13), Hpr6.6, a human homologue found in epithelial tissues (14) and progesterone receptor membrane component-1 (PGRMC1), found in mouse granulosa cells of developing follicles (15). All of these mammalian proteins have nearly identical cytochrome *b<sub>5</sub>* domains, but different C-termini (Figure 1)(16). Recently, both Dap1p and its rat homologue, IZA, have been shown to bind heme when expressed as fusion proteins in *E. coli*. However, their biochemical and spectroscopic characterization is limited to the observation that both fusion proteins display Soret bands at 400 nm, which shift to 420 nm upon reduction with dithionite (6,16). It is remarkable that these proteins bind heme because the two conserved histidine heme ligands found in cytochrome *b<sub>5</sub>* are absent in the MAPR protein family (Figure 1). However, the combined genetic and biochemical data discussed above (6,16), suggest that Dap1p is a heme binding protein, whose heme ligation may be directly related to its function. In the current paper, we have investigated the biochemical and spectroscopic properties of heme binding in both Dap1p and its mouse homologue, mPGRMC1p, in order to determine the nature of the heme ligation and if the manner in which they bind heme is consistent between MAPR's from such evolutionary divergent origins.

## MATERIALS AND METHODS

### Source of Materials

Restriction endonucleases were obtained from New England BioLabs (Beverly, MA). Hemin, sodium dithionite and sodium cyanide were purchased from Sigma. All other reagents were reagent grade or better and were used without further purification.

### Plasmids and Strains

The *E. coli* protein expression plasmids for Dap1p were constructed as follows. The *DAP1* coding sequence flanked with NcoI (5') and XhoI (3') restriction sites was PCR amplified from yeast genomic DNA with two primers (5'-TTTCATGCCATGGGCGAATTCATGTCCTTCATTA AAAACTTG-3' and 5'-CCGCTCGAGTTAAAGCTTTACGTTACGCCAGGCTCCGGTTT-3'). The PCR product was subsequently cloned into vector pET-28a (Novagen) generating the pDap1 plasmid and the *DAP1* gene verified by DNA sequencing.

The *E. coli* protein expression plasmid for the c-terminus, His-tagged, truncated mPGRMC1 protein was constructed, essentially as described above, however the membrane anchor was deleted (residues 1 to 43). The mouse *PGRMC1* coding sequence flanked by NcoI (5') and XhoI (3') restriction sites was PCR amplified from mouse cDNA and cloned into the pET-28a vector, generating the plasmid (pPGRMC1). The *PGRMC1* gene was verified by DNA sequencing and subsequently cut with NcoI/HindIII and ligated into a similarly cut pET-28a

plasmid to generate the C-terminus, His-tagged, membrane anchor-truncated plasmid (pPGRMC1-H6). The primers used were 5'-CAAGCCATGGGCGAATTCAAGATCGTTCGCGGGGACCAG-3' and 5'-CCGCTCGAGTTAAAGCTTTTCATTCTCCGAGCTGTCT-3'.

The Dap1p mutants, Y78F, D118A and Y138F, were generated by site-directed mutagenesis with pDap1, using a Quikchange kit (Stratagene) and the mutations verified by DNA sequencing.

### Expression of Proteins

A single colony of *E. coli* BL21(DE3) bearing either of the above protein expression plasmids was grown in 5 ml L-B broth containing 25 µg/ml kanamycin (FisherBiotech) and reinoculated into 14 L of the same medium. The cultures were grown at 37° C (225 rpms) until an OD<sub>600</sub> of 0.6 was attained. Protein expression was induced by IPTG at 0.5 mM concentration (FisherBiotech) and cells grown overnight at 20° C with 100 rpm shaking.

### Purification of Proteins

The wild-type Dap1 protein (Dap1p) was purified as follows. IPTG-induced cells were harvested by centrifugation and washed. The pellet was re-suspended in 50 mL of 25 mM HEPES buffer, pH 7.5, containing 10% glycerol, 0.1% Triton X-100, and 150 mM NaCl. The cells were disrupted by three bursts of sonication (45 sec) at 4° C. Debris was removed by centrifugation at 27,000 g for 15 min and the pellet re-sonicated as above. Ammonium sulfate was added to the combined supernatants to a concentration of 10%. The solution was centrifuged for 15 mins (27,000 g) and the supernatant collected. The supernatant was brought to a concentration of 40% ammonium sulfate, centrifuged as above, and the pellet was stored in -20° C. The pellet was resuspended in a minimum amount of Milli-Q water (~40% ammonium sulfate final conc.) and loaded directly onto a Macro-Prep methyl hydrophobic column (BioRad), previously equilibrated with 40% ammonium sulfate, 25 mM HEPES, pH 7.5. The column was washed with 3 column volumes of equilibration buffer and the protein was eluted with a linear gradient of water. Fractions with a heme to protein ratio greater than 1 (A<sub>398</sub>/A<sub>280</sub>) were pooled, dialyzed against 25 mM HEPES (pH 7.5) and concentrated in an Amicon pressure concentrator. The concentrated protein was then loaded onto a Superdex-75 gel filtration column (Amersham Biosciences), equilibrated with 25 mM HEPES, pH 7.5, and eluted with the same buffer. It should be noted that two peaks containing Dap1p eluted, one with an approximate size of a tetramer and another, which eluted with the void volume (presumably due to a large aggregate of Dap1p). The area of the tetramer Dap1p peak would decrease if the ammonium sulfate was not completely removed from the sample before loading onto the Superdex-75 column. Fractions were checked for purity by 12% SDS-PAGE stained with Commassie Blue. Greater than 95% pure fractions were pooled and concentrated as above, for a final yield of 6 mg/L of culture (stored with 5% glycerol at -20° C). The mutants of Dap1p (Y78F, D118A and Y138F) were also purified as above.

Bacteria expressing mPGRMC1p-H6 were grown and lysed similarly to Dap1p-expressing cells, described above. The crude lysate was loaded directly onto a Ni-NTA column previously equilibrated with 25 mM HEPES, pH 7.5, 150 mM NaCl and washed with two column volumes of buffer. The protein was eluted with a linear gradient of 500 mM imidazole (250 mM elution for mPGRMC1p-H6). Fractions greater than 95% pure were collected and stored as mentioned above for Dap1p, with a yield of 4 mg/L.

### Oligomeric State Determination

Purified Dap1p and mPGRMC1p-H6 were loaded onto an analytical Superdex 200 size exclusion column (Amersham Biosciences) with a running buffer of 25 mM HEPES pH 7.4,

with and without 150 mM NaCl. The ATKA FPLC system (Amersham Biosciences) was run at a rate of 0.5 ml/min and column was pre-equilibrated with running buffer before each run. A standard protein solution (MP Biomedical, INC.) was used to confirm protein size for Dap1p and mPGRMC1p-H6, which contained apoferritin (480 kDa), gamma-globulin (160 kDa), albumin (67 kDa), ovalbumin (45 kDa), chymotrypsin (25 kDa), cytochrome *c* (13 kDa).

### Mass Spectroscopy

Identification of proteins was confirmed on an Ettan MALDI-ToF/Pro (Amersham Biosciences). A one millimeter gel plug was picked from the SDS-PAGE by an Ettan Spotpicker (Amersham Biosciences), for both Dap1p and mPGRMC1p-H6. The gel plugs were digested overnight with sequencing grade trypsin (Promega) and the peptides extracted with three washes of 75% acetonitrile, 0.1% TFA. The solvent was removed by speed-vac and the peptides were reconstituted in 10  $\mu$ l of 50% acetonitrile, 0.5% TFA, 26 mM alpha-cyano-4-hydroxycinnamic acid. Each peptide solution was spotted twice on the sample slide (0.4  $\mu$ L) and allowed to dry before analysis. The masses of measured peptides were matched with Oracle 9i database through the Ettan MALDI-Tof Pro software 2.0 (Amersham Biosciences).

### Electronic Spectroscopy

UV-Vis spectra of Dap1p and mPGRMC1p-H6 were taken in 25 mM HEPES (pH 7.5) with a Perkin Elmer Lamda 40. All protein samples were reduced by adding excess solid dithionite (10-fold) to the as isolated oxidized samples. Excess cyanide and imidazole (1000-fold each) was added from 7 M stock solutions (in 25 mM HEPES, pH 7.5) to the oxidized proteins to supply exogenous ligands to the iron.

### Percent Heme Loading and Epsilon Determination of Soret band

The percent of heme loading of Dap1p and mPGRMC1p-H6 was determined by the pyridine hemochrome assay (17,18). Briefly, 75  $\mu$ l 1N NaOH, 175  $\mu$ l pyridine, and ~2 mg dithionite were added to 750  $\mu$ l of protein (less than 4  $\mu$ M), and monitored at 418 nm. The heme concentration was determined utilizing the extinction coefficient of 191.5  $\text{mM}^{-1}\text{cm}^{-1}$  at 418 nm for the pyridine-heme adduct. The heme concentration determined for Dap1p and mPGRMC1p-H6 by the pyridine hemochrome assay were then used to determine their Soret band extinction coefficients. Horse heart myoglobin (Mb) (Sigma) was used as standard for both the pyridine hemochrome assay and the extinction coefficient of the Soret band determination (170  $\text{mM}^{-1}\text{cm}^{-1}$  at 408 nm)(19). Protein concentrations were independently determined by Bradford Assay using a horse heart Mb standard.

### Reconstitution of Heme

Reconstitution of Dap1p was performed with the following procedure (20,21). A 1 ml protein solution (1 mg/ml) in 50 mM sodium phosphate buffer (pH 7.0) was added to a three-necked flask and degassed by purging nitrogen for 2–3 h. In a separate round bottom flask, a 10 mM solution of hemin in dimethyl sulfoxide (DMSO) was prepared. This hemin solution was degassed and 1.1 equivalents of hemin was added to the protein solution. DTT was added to a final concentration of 5 mM, using a 0.5 M stock solution, then 300-fold excess to protein of solid dithionite was added and the solution was kept in the dark for overnight at room temperature. The protein was separated from un-complexed heme with a Sephadex G25 column equilibrated with 50 mM sodium phosphate buffer (pH 7.0) at 4 degrees C. Reconstitution of Dap1p with ferric heme was also attempted, where the ferric heme was dissolved in DMSO and titrated into the buffered protein solution at a minimal volume (20).

### Heme Covalency Determination

Dap1p and mPGRMC1p-H6 were digested overnight at 37°C with sequencing grade Trypsin (Promega) and bovine cytochrome *c* was digested as a standard (22). A 100 µl aliquot of the digested protein solutions were loaded on a C4, 300A 4.6 mm × 150 mm column (Western Analytical Products, Inc.) and separated with a step gradient of 62% H<sub>2</sub>O in 0.1% TFA (w/v), 38% acetonitrile in 0.1% TFA (w/v). Free hemin eluted at 16 mins.

### Circular Dichroism (CD) and Fluorescence Spectroscopy

Far-UV spectra of purified Dap1p were obtained on AVIV 60DS CD spectrophotometer. Spectra were recorded using a cuvette having 0.1 mm path length from 250 nm to 190 nm with a step size of 1 nm and an averaging time of 10 s at room temperature. For all spectra an average of six scans were obtained and the background spectra of the buffer was subtracted.

The tryptophan fluorescence spectra were recorded by Perkin-Elmer Luminescence Spectrometer LS 50B. Dap1p (10 µM) was excited at 295 nm and the emission was scanned from 330 to 400 nm in 50 mM phosphate (pH 7.0) buffer solution.

### EPR Spectroscopy

The EPR spectra of Dap1p (8 mg/ml) and mPGRMC1p-H6 (10.4 mg/ml), all in 25 mM HEPES (pH 7.5) were recorded with a Bruker Elexsys/ Oxford Cryostat EPR (0-8000 gauss, 8 G modulation amplitude, 0.2 mW, 9.63 GHz and 4 degrees K). Sodium cyanide and imidazole were added to the individual samples (1µL of a 7 M stock solutions) to get a final concentration of 35 mM. Horse heart Mb (Sigma) was used as a standard (0.4 mg/ml)

### Magnetic Circular Dichroism (MCD) Measurements

MCD measurements were made at 22 °C on an 62DS circular dichroism spectrophotometer (Aviv, Lakewood, NJ) equipped with a 0.64 T permanent magnet (model PM-2, Jasco, Eaton, MD). Samples of Dap1p, Y78F and D118A, containing heme concentrations of 80, 100 and 70 µM, respectively, in 25 mM HEPES buffer (pH 7.5), were placed in a 1-mm path length cylindrical quartz cell. MCD spectra were calculated from the difference between parallel and antiparallel field measurements, baseline corrected and smoothed (23-point Savitzky-Golay algorithm).

## RESULTS AND ANALYSIS

### Expression and Purification

Dap1p, Y78F, D118A, Y138F and mPGRMC1p-H6 were expressed in an *E. coli* strain (BL21-DE3) to high levels. Dap1p, Y78F, D118A and Y138F were purified by ammonium sulfate precipitation, a hydrophobic column, and a gel filtration column for a final yield of approximately 6 mg/L. mPGRMC1p-H6 was purified by a Ni-NTA agarose affinity column for a yield of approximately 4 mg/L.

### Oligomeric State Determination of Dap1p

Dap1p appeared to run as a multimer on the Superdex-75 column during purification, therefore, purified Dap1p and mPGRMC1p-H6 samples were analyzed on an analytical Superdex 200 size exclusion column (SEC) to measure their asisolated size more accurately. Initial analysis of purified Dap1p and mPGRMC1p-H6 in 25 mM HEPES (pH 7.4) showed a single peak at ~68 kDa (a possible tetramer), as compared to protein standards (Figure 2). Addition of DTT, CHAPS, or Triton-X caused an aggregation of Dap1p to a large multimer between 480-160 kDa. Addition of 150 mM NaCl to Dap1p, however, reduced the tetramer to a dimer, which

ran as ~34 kDa (Figure 2). Addition of excess DTT to Dap1p could not reduce the dimer to monomer on the analytical SEC.

### Mass Spectroscopy

Samples of SDS-PAGE isolated, trypsin-digested Dap1p and mPGRMC1p-H6 samples were identified by MALDI-ToF. Both of their expectation values were 0.000 and their coverage was greater than 55%. Seven out of twenty-two peaks and six of sixteen were assigned to expected peptides of Dap1p and mPGRMC1p-H6, respectively.

### Electronic Spectroscopy

The UV- visible spectra of Dap1p (Figure 3) displays a maxima at 398 nm, characteristic of a hemoprotein Soret band, with three additional bands at 500, 530 and 620 nm (mPGRMC1p-H6 shows the same absorption spectra, data not shown). The small peak near 620 nm has been designated as the charge transfer band between the heme and the high spin Fe(III) (23). Upon reduction with excess dithionite the Soret bands from both Dap1p and mPGRMC1p-H6 underwent a red shift to 418 nm, with two new bands at 538 and 562 nm, corresponding to the  $\beta$  and  $\alpha$  heme bands, respectively. These data are consistent with a high-spin, 5-coordinate ferric heme center for both Dap1p and mPGRMC1p-H6, as isolated (24–26). Addition of imidazole to the ferric heme protein shifts the Soret band from 398 nm to 407 nm and decreases the intensity of the 620 nm band for Dap1p. Addition of excess  $\text{CN}^-$  to the solution of Dap1p gave rise to a red shifted Soret band (398 to 421 nm) and an additional broad band at 545 nm. These changes in the electronic spectra are consistent with both imidazole and  $\text{CN}^-$  binding directly to the iron, generating a 6-coordinate, low-spin Fe(III) (27,28).

### Percent Heme Loading and Epsilon Determination of the Soret band

The pyridine hemochrome assay determined the heme content of Dap1p to be 17 % (highest value of 3 purifications) and that of mPGRMC1p-H6 to be 21 % (highest value of 3 purifications) (17,18). The heme loading for the Dap1p mutants were as follows: Y78F (7 %), D118A (25 %) and Y138F (0 %), (highest value of 2 purifications). Utilizing the pyridine hemochrome assay, the extinction coefficient of the Soret band at 398 nm for Dap1p was calculated to be  $99 \pm 4.1 \text{ mM}^{-1}\text{cm}^{-1}$  and  $102 \pm 3.5 \text{ mM}^{-1}\text{cm}^{-1}$  for mPGRMC1p-H6. The extinction coefficient values of the Heme  $\pi \rightarrow \pi^*$  Soret transition for Dap1p and mPGRMC1p-H6 are close to the lower limit of the values described in the literature for hemoproteins ( $100\text{--}200 \text{ mM}^{-1}\text{cm}^{-1}$ ) (29).

### Reconstitution of Heme

Reconstitution of the 17 % heme loaded Dap1p with ferrous heme increased the heme content to a maximum of 27%, while reconstitution with ferric heme was unsuccessful in increasing the heme content of Dap1p. Reconstitution under buffer conditions where Dap1p was a dimer (150 mM salt) also did not improve the percent loading of heme. Reconstitution was attempted under various other conditions such as varying pH and denaturant (urea and guanidinium HCl) with no success.

### Heme Covalency

Dap1p and mPGRMC1p-H6 were both digested with trypsin and their fragments were separated by HPLC, with the peptide backbone (215 nm), aromatic side chains (280 nm), and heme (400 nm) monitored simultaneously. Only one peak was detected at 400 nm and eluted at 16 mins for both Dap1p and mPGRMC1p-H6. This corresponds to the elution time for free heme and indicates the heme is not covalently attached to Dap1p or mPGRMC1p-H6. This result differs from that of the control, cytochrome *c*, which displayed a protein-heme peak that eluted at 14 mins (22).

## Circular Dichroism (CD) and Fluorescence Spectroscopy

The Far-UV CD spectra of Dap1p shows characteristic features near 222 nm, 208 nm and 192 nm with a 190/222 ratio of 1.6, which indicate that the protein has alpha helical secondary structure (30). In the fluorescence spectra of Dap1p, the tryptophan maxima was observed at 341 nm, indicating that the tryptophans of Dap1p are partially buried. For comparison, free, solvent exposed tryptophan gave a maxima of 355 nm.

## EPR Spectroscopy

Dap1p, mPGRMC1p-H6 and heme-reconstituted Dap1p all display identical EPR spectra, with a strong derivative signal centered at  $g \sim 6$  ( $g$ -values of 6.40 and 5.59) and a smaller negative signal at  $g = 1.99$ , which clearly indicate an axial Fe(III) high spin species ( $E/D = 0.017$ ) (Figure 4). The signals of both Dap1p and mPGRMC1p-H6 were integrated by comparing the signal area with that of a similar heme concentration of horse heart Mb, which confirmed the approximate heme content determined by the pyridine hemochrome assay (the zero-field splitting of Dap1p and mPGRMC1p-H6 were assumed to be comparable to that of myoglobin). Addition of excess  $CN^-$  gave EPR signals with  $g$ -values of 2.97, and 2.22 for Dap1p and 2.90 and 2.23 for mPGRMC1p-H6. Addition of excess imidazole to Dap1p gave an EPR spectra with  $g$  values of 2.26 and 2.96, whereas the two  $g$ -values for mPGRMC1p-H6 were 2.26 and 2.98 (the third  $g$ -value for both the imidazole and cyanide adducts was distorted by a minor copper impurity at  $g = 2$ ).

## MCD Spectroscopy

The MCD spectrum of ferric Dap1p in the Soret and visible band spectral regions (Figure 5) contains several features providing a "fingerprint" that can aid in characterizing the nature of the heme axial ligand. A "W" shaped feature of modest intensity (magnitudes of  $3\text{--}5\text{ M}^{-1}\text{ cm}^{-1}\text{ T}^{-1}$ ) in the Soret region contains troughs at 397 and 429 nm separated by a central peak at 412 nm and is bordered on the lower wavelength side by a peak at 376 nm. In the visible region, peaks at 478, 525, and 604 nm are interlaced with troughs at 505, 555, and 643 nm. The spectra of Y78F and D118A were comparable to Dap1p, with only negligible differences.

## DISCUSSION

Dap1 has recently been shown to bind heme and is apparently critical to Erg1p stability, however, its physiological role remains undetermined (6). Work by others and our unpublished biological studies, indicate that Dap1p may function in a heme-dependent mechanism (6,7). As part of our ongoing effort to determine the role of Dap1p and its mechanism of action, we expressed and purified Dap1p and its mouse homolog, mPGRMC1p-H6, and conducted biochemical investigations in the hope of shedding some light on their specific biological function. In this regard, our investigations have revealed several novel aspects about how Dap1p and mPGRMC1p-H6 may function. First, we have found that Dap1p is a dimer at physiological salt concentrations, similar to that observed for IZA (16), but it has a propensity to form tetramers at lower salt concentrations. Second, both Dap1p and mPGRMC1p-H6 bind heme non-covalently. Considering that IZA also binds heme and there is 98% sequence homology between mPGRMC1p and IZA and a 57% sequence homology between Dap1p and IZA, heme binding appears to be a common characteristic to this family of proteins. Third, Dap1p and mPGRMC1p-H6 bind heme with a low loading percentage, 17% and 21%, respectively, suggesting the low heme content may also be a common trait of this novel protein family. The heme loading percentage for Dap1p can be increased to 27% by incubation with ferrous heme and is independent of the multimeric state of the protein (ie. dimer versus tetramer). The low heme content for Dap1p and mPGRMC1p-H6 is most likely not due to their expression in *E. coli* since other hemoproteins can be fully loaded with heme (31–33), nor due to mis-folded protein since both CD and fluorescence spectroscopy indicate Dap1p has a well-

ordered structure. This low heme content in a well-ordered protein is notable because of Dap1p's sequence similarity to Cytochrome *b*<sub>5</sub>, a tight heme binding protein with two His ligands to the heme. Considering that these proximal histidine ligands are not conserved in Dap1p, it is clear that Dap1p binds heme with different axial ligand(s) than cytochrome *b*<sub>5</sub>, which could explain its low heme loading. Interestingly, the NMR structure of the plant MAPR, At2g24940.1, did not have heme bound even though there was a cleft for potential heme binding in the structure (34). The lack of heme binding could be explained by the fact that the protein was expressed *in vitro* with wheat germ extract, which would not provide a heme cofactor for binding.

The electronic spectra of both Dap1p and mPGRMC1p-H6 in the oxidized and reduced states indicate a high spin, 5-coordinate heme environment, in contrast to the low spin, 6-coordinate heme environment found in cytochrome *b*<sub>5</sub> (24,25). In terms of both absorption peak position and amplitudes in the Soret,  $\alpha/\beta$  and charge-transfer transitions, the optical spectra of Dap1p and mPGRMC1p-H6 are similar to both histidine ligated proteins (i.e. met-myoglobin and prostaglandin H synthase) and tyrosine ligated proteins (i.e. catalase) (27), which makes it difficult to determine the nature of the axial ligand. A low spin, 6-coordinate species could be generated for both Dap1p and mPGRMC1p-H6 with the addition of cyanide and imidazole, as seen by the change in UV-vis spectra, indicating either an empty coordination site or an easily displaced ligand, such as exogenous water. The high spin, 5-coordinate ligand environment for the ferric Dap1p and mPGRMC1p-H6 is corroborated by its EPR spectrum, which manifests an axial, ferric signal ( $E/D = 0.017$ ). The  $E/D$  value and rhombicity index,  $R$  ( $R = [(\Delta g/16) \times 100] = 5.1\%$ , where  $\Delta g$  is the absolute difference between the two  $g$ -values centered at  $g = 6$ ), for both Dap1p and mPGRMC1p-H6 are very similar to the signals of horseradish peroxidase (pH 8.1) (35) and cytochrome-c peroxidase (pH 5)(36), suggesting an axial His and a bound water (or open coordination site). The assignment of an axial His is supported by the low spin, EPR signal observed after addition of exogenous imidazole ( $g$ -values of 2.26 and 2.96), similar to that observed for hemoglobin (37). Nevertheless, this analysis is in contrast with the fact that there are no conserved histidines in the MAPR protein family that could function as the axial ligand in Dap1p or mPGRMC1p-H6. Considering that the rhombicity index is a poor indicator of the axial ligation (27) and that the added imidazole could possibly displace the endogenous axial ligand, generating a bis-imidizolate complex, another spectroscopic method was required to identify the nature of the axial ligand.

MCD spectroscopy is an extremely sensitive method of investigating heme proteins and provides more reliable information about the heme state and axial ligands than EPR or simple optical spectra (38,39). Coordination differences, while not apparent in the UV-Vis absorption spectra, are more obvious from the differences in their respective MCD spectra. MCD spectra can have negative and positive absorptions, which provide considerably more fine structure than can be seen in absorption spectra alone. Therefore, empirical comparisons of MCD spectra contain twice the information (i.e., intensity and sign) and thus provide better "fingerprints" than UV-Vis absorption alone. In this regard, the MCD spectrum of Dap1p is clearly not consistent with histidine as the axial ligand, lacking the more intense "S" shaped feature centered near 412 nm as seen in the spectra of both ferric myoglobin, having a histidine residue as the fifth ligand and water as the sixth (peak amplitude of  $14 \text{ M}^{-1} \text{ cm}^{-1} \text{ T}^{-1}$ ) (40,41), and in ferric cytochrome *b*<sub>5</sub>, having bis-histidine axial coordination (peak amplitude of  $68 \text{ M}^{-1} \text{ cm}^{-1} \text{ T}^{-1}$ ) (42). Nor does the spectrum of Dap1p resemble the spectrum observed in high-spin ferric horseradish peroxidase, which has proximal histidine coordination without a water as the sixth ligand (41). The spectrum is also not consistent with cysteine ligation due to the absence of the prominent, single trough at 395 nm (peak amplitude of  $-25 \text{ M}^{-1} \text{ cm}^{-1} \text{ T}^{-1}$ ) (43). The MCD spectrum of Dap1p is more consistent in the visible region with spectra observed in heme proteins (44) and model compounds (45) having carboxylate heme coordination, but their Soret region spectral features do not correspond well with the Dap1p



spectrum. For example, the central Soret peak of heme oxygenase H25A (assigned heme-glutamate coordination) is red shifted by 20 nm to 392 nm and the short wavelength trough is red shifted by 40 nm to 358 nm when compared with the corresponding features in Dap1p (44). However, a remarkably close match to both the Soret and visible band MCD of Dap1p is found in the MCD of the catalases, a family of heme proteins that catalyze the disproportionation of hydrogen peroxide and have an axial tyrosine ligation (Figure 5)(46–49). X-ray crystallography of bovine liver catalase shows that not only is the heme axially coordinated by a tyrosine residue (presumably in the form of tyrosinate), but that the tyrosine hydroxyl oxygen is also hydrogen bonded by a nearby arginine residue (50). It is tempting to speculate that the presence of this hydrogen bond to the heme axial ligand may explain why the MCD spectra of the catalases are distinguished from those of other tyrosine-heme coordinated examples lacking this hydrogen bond, such as Mb H93Y or heme-phenolate model compounds (44,51).

As stated previously, the MAPR family of proteins does not contain the conserved histidine ligands of cytochrome *b*<sub>5</sub> but they do have a conserved tyrosine and aspartic acid adjacent to the histidine positions cytochrome *b*<sub>5</sub> (Tyr78 and Asp118 in Figure 1). These two candidates for ligation were subsequently mutated (Y78F and D118A), however, both mutant proteins still bound heme and there was minimal change in their MCD spectra compared to Dap1p. We therefore considered other conserved tyrosine residues as potential axial ligands and one, Y138F, had no bound heme after purification. These results indicate that Tyr138 is the axial ligand to the heme for Dap1p, confirming the MCD spectroscopy. If one assumes the structure of Dap1p is comparable to the NMR structure of its plant homologue, At2g24940.1 (63% sequence homologous), one observes that the conserved tyrosine (Tyr138 in Dap1p and Tyr92 in At2g24940.1) is positioned on the edge of the hydrophobic cleft and could potentially bind a heme cofactor. Considering that this tyrosine is conserved in all MAPR's, it is highly likely that this tyrosine is the axial ligand for both mPGRMC1 (Tyr164) and IZA (Tyr164), as well. Interestingly, there is a conserved lysine adjacent to this tyrosine, which could hydrogen bond and account for the “catalase-like” MCD spectrum.

The biological function(s) of MAPR proteins is still unclear with regards to heme (6,16) and/or sterol (9,10) binding. The most extensive data to date comes from the study of the yeast MAPR, Dap1p, which support a role for heme binding in its biological function. The fact that Dap1p has high sequence homology with cytochrome *b*<sub>5</sub> but ligates heme in a different manner may also have relevance to its biological function. Previously, it was observed that exogenous heme in the yeast media can correct the *dap1Δ* phenotype and restore the Erg11p stability (6), however, as yeast can degrade heme and release iron via heme oxygenase (Hmx1p), this experiment can not differentiate between heme and iron. In this study, mutating Asp91 in Dap1p, a conserved residue in all MAPR and cytochrome *b*<sub>5</sub> proteins, abolished heme binding in Dap1p and did not complement the MMS sensitivity phenotype of the *dap1Δ* strain. This result was interpreted as meaning that heme binding was critical to Dap1p function, however, it should be noted that the Asp91 mutant was not conclusively proven to be properly folded while attached to the GST fusion protein (6). In addition, the amount of Erg11p was lowered in the *dap1Δ* strain but the transcription of *ERG11* was not, indicating that Dap1p does not play a role in transcriptional activation. Based on the data reported here and the literature, there are two probable roles for Dap1p with heme. First, Dap1p might play a role in cellular heme synthesis or transport, therefore, indirectly affecting Erg11p stability. Consistent with this idea, the *dap1Δ* mutant has a transcriptional profile, similar to heme synthesis pathway mutants (7). Another possibility is that Dap1p may play a role as a heme chaperone to Erg11p, thus modulating the stability of Erg11p by delivering its essential cofactor, heme, and consequently increasing its activity in sterol synthesis. The existence of apo-Dap1p along with heme-bound Dap1p under physiological conditions may allow Dap1p to function as a ‘Heme-stat’ to gauge cellular heme status and in turn modulate Erg11p level and its activity. Mallory et al. did not

detect a physical interaction between Dap1p and Erg11p by immunoprecipitation, however, this negative result could be due to the fact that the Dap1p-Erg11p interaction is transient, similar to the interaction between the copper chaperone, Atx1p, and its target, Ccc2p, in yeast (52). Both of these possible roles of heme and Dap1p are currently under investigation.

In summary, the current data indicates that both Dap1 and mPRGMC1-H6 bind heme in a similar 5-coordinate manner, with tyrosine as the axial ligand (Tyr138 for Dap1p) but they are not 100% loaded with heme. Given the fact that we now have identified the exact axial ligand for Dap1p, we are currently conducting both genetic and biochemical studies to investigate the biological roles of Dap1p and mPGRMC1p and whether heme binding is critical for their function as suggested in the literature.

## ABBREVIATIONS

Dap1p, Yeast Dap1 protein  
 mPGRMC1p, mouse progesterone receptor membrane component-1 protein  
 mPGRMC1p-H6, C-terminus, His-tagged, membrane anchor-truncated mPGRMC1p  
 MAPR, membrane-associated progesterone binding protein  
 IZA, inner zone antigen  
 GST, glutathione S-transferase  
 EPR, electron paramagnetic resonance  
 MCD, magnetic circular dichroism  
 CD, circular dichroism  
 Y78F, Dap1p-Tyr78Phe  
 D118A, Dap1p-Asp118Ala  
 Y138F, Dap1p-Tyr138Phe  
 MMS, methyl methanesulfonate  
 SEC, size exclusion column  
 Mb, myoglobin  
 MALDI-ToF, matrix assisted laser desorption ionization time-of-flight  
 FPLC, fast protein liquid chromatography

## ACKNOWLEDGEMENTS

We acknowledge Prof. M. Jurica for the use of her analytical SEC column, Prof. Brian Gibney for valuable discussions and Kate Chabarek, Micheal Eklund and Pilgrim Jackson for valuable assistance.

## REFERENCES

1. Begley TJ, Rosenbach AS, Ideker T, Samson LD. Damage recovery pathways in *Saccharomyces cerevisiae* revealed by genomic phenotyping and interactome mapping. *Mol Cancer Res* 2002;1:103–112. [PubMed: 12496357]
2. Hand RA, Jia N, Bard M, Craven RJ. *Saccharomyces cerevisiae* Dap1p, a novel DNA damage response protein related to the mammalian membrane-associated progesterone receptor. *Eukaryot Cell* 2003;2:306–317. [PubMed: 12684380]
3. Game JC. The *Saccharomyces* repair genes at the end of the century. *Mutat Res* 2000;451:277–293. [PubMed: 10915878]
4. Myung K, Kolodner RD. Suppression of genome instability by redundant S-phase checkpoint pathways in *Saccharomyces cerevisiae*. *Proc Natl Acad Sci U S A* 2002;99:4500–4507. [PubMed: 11917116]
5. Prakash S, Prakash L. Increased spontaneous mitotic segregation in MMS-sensitive mutants of *Saccharomyces cerevisiae*. *Genetics* 1977;87:229–236. [PubMed: 200524]
6. Mallory JC, Crudden G, Johnson BL, Mo C, Pierson CA, Bard M, Craven RJ. Dap1p, a Heme-Binding Protein That Regulates the Cytochrome P450 Protein Erg11p/Cyp51p in *Saccharomyces cerevisiae*. *Molecular and Cellular Biology* 2005;25:1669–1679. [PubMed: 15713626]

7. Vulpe C, Oh E. 2005 Unpublished Results
8. Mifsud W, Bateman A. Membrane-bound progesterone receptors contain a cytochrome b5-like ligand-binding domain. *Genome Biol* 2002;3:1–5. RESEARCH0068
9. Meyer C, Schmid R, Schmieding K, Falkenstein E, Wehling M. Characterization of high affinity progesterone-binding membrane proteins by anti-peptide antiserum. *Steroids* 1998;63:111–116. [PubMed: 9516722]
10. Krebs CJ, Jarvis ED, Chan J, Lydon JP, Ogawa S, Pfaff DW. A membrane-associated progesterone-binding protein, 25-Dx, is regulated by progesterone in brain regions involved in female reproductive behaviors. *Proc Natl Acad Sci U S A* 2000;97:12816–12821. [PubMed: 11070092]
11. Runko E, Wideman C, Kaprielian Z. Cloning and expression of VEMA: a novel ventral midline antigen in the rat CNS. *Mol Cell Neurosci* 1999;14:428–443. [PubMed: 10656251]
12. Nolte I, Jeckel D, Wieland FT, Sohn K. Localization and topology of ratp28, a member of a novel family of putative steroid-binding proteins. *Biochim Biophys Acta* 2000;1543:123–130. [PubMed: 11087948]
13. Raza FS, Takemori H, Tojo H, Okamoto M, Vinson GP. Identification of the rat adrenal zona fasciculata/reticularis specific protein, inner zone antigen (IZAg), as the putative membrane progesterone receptor. *Eur J Biochem* 2001;268:2141–2147. [PubMed: 11277938]
14. Hand RA, Craven RJ. Hpr6.6 protein mediates cell death from oxidative damage in MCF-7 human breast cancer cells. *J Cell Biochem* 2003;90:534–547. [PubMed: 14523988]
15. Peluso JJ, Pappalardo A, Losel R, Wehling M. Expression and function of PAIRBP1 within gonadotropin-primed immature rat ovaries: PAIRBP1 regulation of granulosa and luteal cell viability. *Biol Reprod* 2005;73:261–270. [PubMed: 15814896]
16. Min L, Takemori H, Nonaka Y, Katoh Y, Doi J, Horike N, Osamu H, Raza FS, Vinson GP, Okamoto M. Characterization of the adrenal-specific antigen IZA (inner zone antigen) and its role in the steroidogenesis. *Mol Cell Endocrinol* 2004;215:143–148. [PubMed: 15026187]
17. Paul KG, Theorell H, Akeson A. The molar light absorption of pyridine ferroprotoporphyrin. *Acta Chem. Scand* 1953;7:1284–1287.
18. Furhrhop, J-H.; Smith, KM. *Laboratory Methods in Porphyrin and Metalloporphyrin Research*. Amsterdam: New York: Elsevier Scientific Publishing Co.; 1975.
19. Blum O, Haiek A, Cwikel D, Dori Z, Meade TJ, Gray HB. Isolation of a myoglobin molten globule by selective cobalt(III)-induced unfolding. *Proc Natl Acad Sci U S A* 1998;95:6659–6662. [PubMed: 9618468]
20. Daltrop O, Stevens JM, Higham CW, Ferguson SJ. The CcmE protein of the c-type cytochrome biogenesis system: unusual in vitro heme incorporation into apo-CcmE and transfer from holo-CcmE to apo-cytochrome. *Proc Natl Acad Sci U S A* 2002;99:9703–9708. [PubMed: 12119398]
21. Stevens JM, Daltrop O, Higham CW, Ferguson SJ. Interaction of heme with variants of the heme chaperone CcmE carrying active site mutations and a cleavable N-terminal His tag. *J Biol Chem* 2003;278:20500–20506. [PubMed: 12657624]
22. Schulz H, Hennecke H, Thony-Meyer L. Prototype of a heme chaperone essential for cytochrome c maturation. *Science* 1998;281:1197–1200. [PubMed: 9712585]
23. Bartalesi I, Bertini I, Ghosh K, Rosato A, Turano P. The unfolding of oxidized c-type cytochromes: the instructive case of *Bacillus pasteurii*. *J Mol Biol* 2002;321:693–701. [PubMed: 12206783]
24. Lever, ABP.; Gray, HB. *Iron Porphyrins, Part I*. Reading, Massachusetts: Addison-Wesley Publishing Co.; 1983.
25. Pettigrew, GW.; Moore, GR. *Cytochrome c, Biological Aspects*. Berlin: Springer-Verlag; 1987.
26. Smulevich G, Neri F, Willemsen O, Choudhury K, Marzocchi MP, Poulos TL. Effect of the His175→Glu mutation on the heme pocket architecture of cytochrome c peroxidase. *Biochemistry* 1995;34:13485–13490. [PubMed: 7577937]
27. Tsai AL, Kulmacz RJ, Wang JS, Wang Y, Van Wart HE, Palmer G. Heme coordination of prostaglandin H synthase. *J Biol Chem* 1993;268:8554–8563. [PubMed: 8386163]
28. Kulmacz RJ, Tsai AL, Palmer G. Heme spin states and peroxide-induced radical species in prostaglandin H synthase. *J Biol Chem* 1987;262:10524–10531. [PubMed: 3038886]

29. Moore, GR.; Pettigrew, GW. Cytochromes c - Evolutionary Structural and Physicochemical Aspects. Springer-Verlag; 1990.
30. Padmanabhan S, Marqusee S, Ridgeway T, Laue TM, Baldwin RL. Relative helix-forming tendencies of nonpolar amino acids. *Nature* 1990;344:268–270. [PubMed: 2314462]
31. Beck von Bodman S, Schuler MA, Jollie DR, Sligar SG. Synthesis, bacterial expression, and mutagenesis of the gene coding for mammalian cytochrome b5. *Proc Natl Acad Sci U S A* 1986;83:9443–9447. [PubMed: 3540940]
32. Arnesano F, Banci L, Bertini I, Felli IC. The solution structure of oxidized rat microsomal cytochrome b5. *Biochemistry* 1998;37:173–184. [PubMed: 9425037]
33. Bertini I, Luchinat C, Turano P, Battaini G, Casella L. The magnetic properties of myoglobin as studied by NMR spectroscopy. *Chemistry* 2003;9:2316–2322. [PubMed: 12772306]
34. Song J, Vinarov D, Tyler EM, Shahan MN, Tyler RC, Markley JL. Hypothetical protein At2g24940.1 from *Arabidopsis thaliana* has a cytochrome b5 like fold. *J Biomol NMR* 2004;30:215–218. [PubMed: 15702529]
35. Blumberg WE, Peisach J, Wittenberg BA, Wittenberg JB. The electronic structure of protoheme proteins. I. An electron paramagnetic resonance and optical study of horseradish peroxidase and its derivatives. *J Biol Chem* 1968;243:1854–1862. [PubMed: 5646479]
36. Wittenberg BA, Kampa L, Wittenberg JB, Blumberg WE, Peisach J. The electronic structure of protoheme proteins. II. An electron paramagnetic resonance and optical study of cytochrome c peroxidase and its derivatives. *J Biol Chem* 1968;243:1863–1870. [PubMed: 5646480]
37. Ikeda-Saito M, Iizuka T. Studies on the heme environment of horse heart ferric cytochrome c. Azide and imidazole complexes of ferric cytochrome c. *Biochim Biophys Acta* 1975;393:335–342. [PubMed: 167834]
38. Sutherland JC, Holmquist B. Magnetic circular dichroism of biological molecules. *Annu Rev Biophys Bioeng* 1980;9:293–326. [PubMed: 6249185]
39. Hatano M, Nozawa T. Magnetic circular dichroism approach to hemoprotein analyses. *Adv Biophys* 1978;11:95–149. [PubMed: 354350]
40. Vickery L, Nozawa T, Sauer K. Magnetic circular dichroism studies of myoglobin complexes. Correlations with heme spin state and axial ligation. *J Am Chem Soc* 1976;98:343–350. [PubMed: 173751]
41. Dawson JH, Kadkhodayan S, Zhuang C, Sono M. On the use of iron octa-alkylporphyrins as models for protoporphyrin IX-containing heme systems in studies employing magnetic circular dichroism spectroscopy. *J Inorg Biochem* 1992;45:179–192. [PubMed: 1634892]
42. Vickery L, Salmon A, Sauer K. Magnetic circular dichroism studies on microsomal aryl hydrocarbon hydroxylase: comparison with cytochrome b-5 and cytochrome P-450-cam. *Biochim Biophys Acta* 1975;386:87–98. [PubMed: 164936]
43. Sono M, Stuehr DJ, Ikeda-Saito M, Dawson JH. Identification of nitric oxide synthase as a thiolate-ligated heme protein using magnetic circular dichroism spectroscopy. Comparison with cytochrome P-450-CAM and chloroperoxidase. *J Biol Chem* 1995;270:19943–19948. [PubMed: 7544348]
44. Pond AE, Roach MP, Sono M, Rux AH, Franzen S, Hu R, Thomas MR, Wilks A, Dou Y, Ikeda-Saito M, Ortiz de Montellano PR, Woodruff WH, Boxer SG, Dawson JH. Assignment of the heme axial ligand(s) for the ferric myoglobin (H93G) and heme oxygenase (H25A) cavity mutants as oxygen donors using magnetic circular dichroism. *Biochemistry* 1999;38:7601–7608. [PubMed: 10360958]
45. Nozawa T, Ookubo S, Hatano M. Visible and near-infrared MCD spectra of h.s. iron(III) complexes of protoporphyrin-IX-dimethylester. *J. Inorg. Biochem* 1980;12:253–267.
46. Abraham BD, Sono M, Boutaud O, Shriner A, Dawson JH, Brash AR, Gaffney BJ. Characterization of the coral allene oxide synthase active site with UV-visible absorption, magnetic circular dichroism, and electron paramagnetic resonance spectroscopy: evidence for tyrosinate ligation to the ferric enzyme heme iron. *Biochemistry* 2001;40:2251–2259. [PubMed: 11329294]
47. Andersson LA, Johnson AK, Simms MD, Willingham TR. Comparative analysis of catalases: spectral evidence against heme-bound water for the solution enzymes. *FEBS Lett* 1995;370:97–100. [PubMed: 7649312]

48. Eglinton DG, Gadsby PM, Sievers G, Peterson J, Thomson AJ. A comparative study of the low-temperature magnetic circular dichroism spectra of horse heart metmyoglobin and bovine liver catalase derivatives. *Biochim Biophys Acta* 1983;742:648–658. [PubMed: 6838894]
49. Browett WR, Stillman MJ. Magnetic circular dichroism studies of bovine liver catalase. *Biochim Biophys Acta* 1979;577:291–306. [PubMed: 36920]
50. Fita I, Rossmann MG. The active center of catalase. *J Mol Biol* 1985;185:21–37. [PubMed: 4046038]
51. Roach MP, Puspita WJ, Watanabe Y. Proximal ligand control of heme iron coordination structure and reactivity with hydrogen peroxide: investigations of the myoglobin cavity mutant H93G with unnatural oxygen donor proximal ligands. *J Inorg Biochem* 2000;81:173–182. [PubMed: 11051562]
52. Pufahl RA, Singer CP, Peariso KL, Lin SJ, Schmidt PJ, Fahrni CJ, Culotta VC, Penner-Hahn JE, O'Halloran TV. Metal ion chaperone function of the soluble Cu(I) receptor Atx1. *Science* 1997;278:853–856. [PubMed: 9346482]

**Figure 1.**

Alignment of IZA (accession number CAA06732), mPGRMC1p (accession number NP\_058063), Hpr6.6 (accession number NP\_006658), Dap1p (accession number Q12091), and the cytochrome  $b_5$  binding motif (pfam00173) using Clustal W v1.82. Conserved amino acid residues that have been mutated in Dap1p are shaded in black and numbers above correspond to the Dap1p sequence. Axial heme ligating histidines from cytochrome  $b_5$  are also highlighted, for comparison. The single predicted transmembrane segment is indicated above residues involved. This prediction is based on a Kyte-Doolittle hydropathy plot with a window size of 9. Fully conserved residues are indicated with “\*”, strongly conserved amino acids with “:”, and weakly conserved residues with “.”.

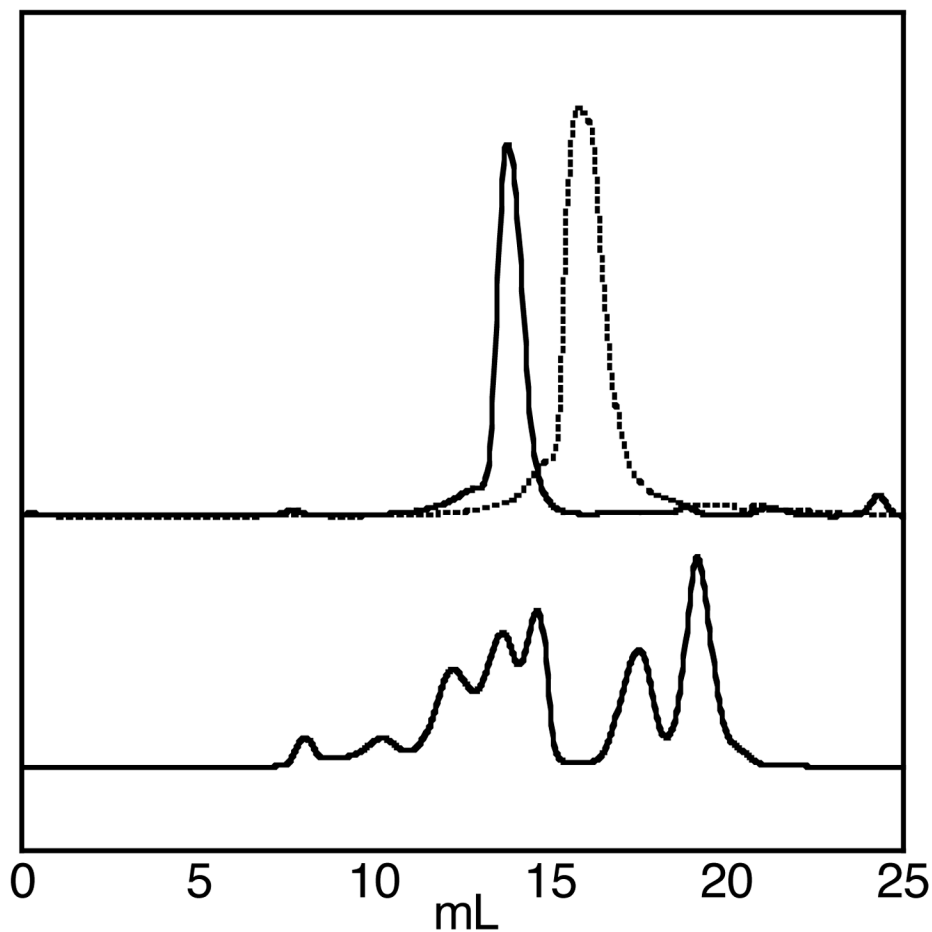


**Figure 2.** HPLC traces of the analytical size exclusion column. Top traces are that of Dap1p (solid line, no salt) and Dap1p (dashed line, 150 mM salt). Bottom trace is that of protein standards. The first peak is the void volume, then apoferritin (480 kDa), gamma-globulin (160 kDa), albumin (67 kDa), ovalbumin (45 kDa), chymotrypsin (25 kDa), cytochrome *c* (13 kDa).

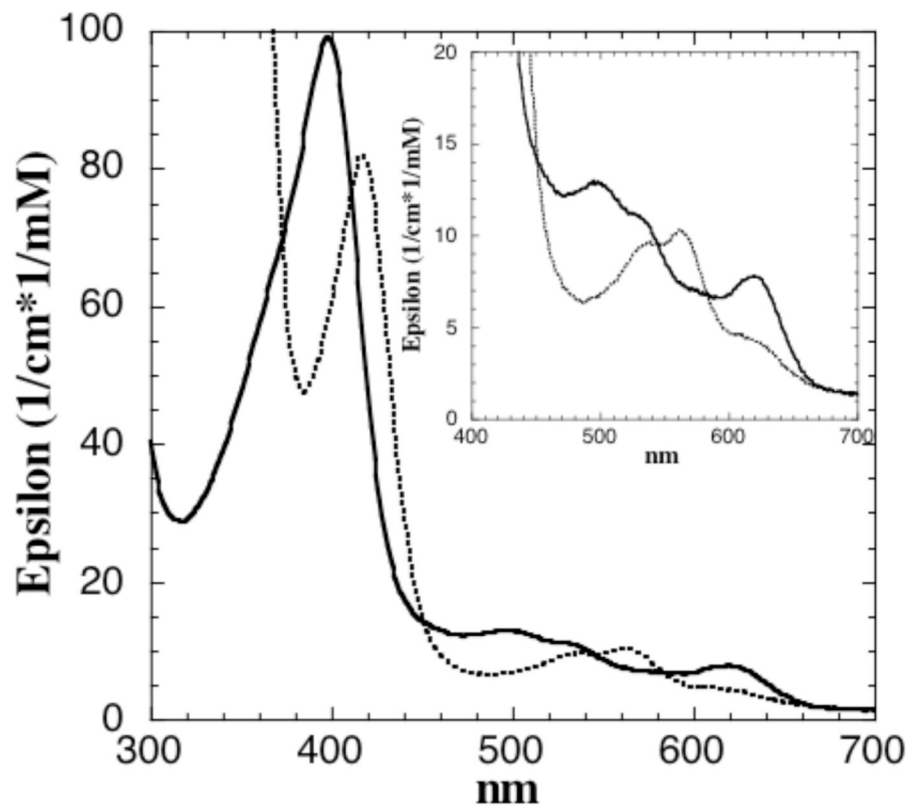


**Figure 3.** UV-visible spectra of oxidized (solid) and reduced (dashed) Dap1p. Inset is an enhancement of the far-visible spectrum. The large absorbance at 300 nm for the reduced spectrum is that of excess sodium dithionite.



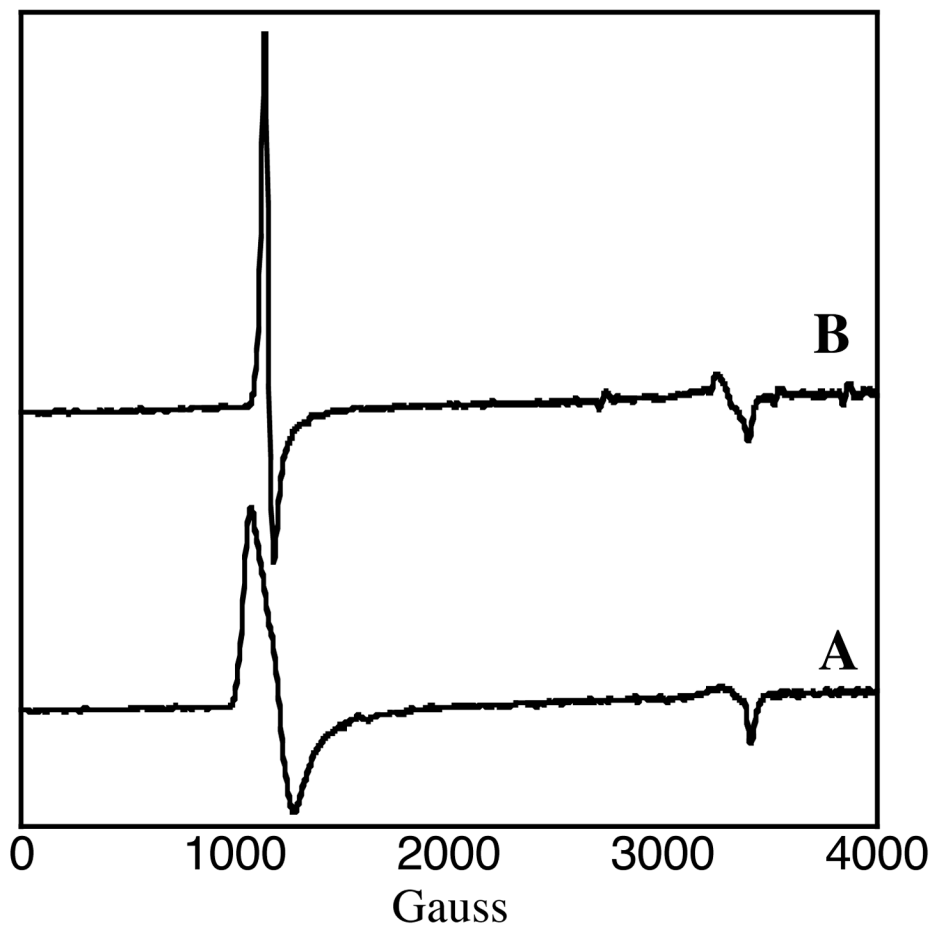


**Figure 4.** EPR spectra of (A) Dap1p (8 mg/ml, HEPES, pH 7.5) and (B) horse heart myoglobin (0.4 mg/ml, HEPES, pH 7.5). EPR parameters: 0-8000 gauss, 8 G modulation amplitude, 0.2 mW, 9.63 GHz and 4 degrees K.

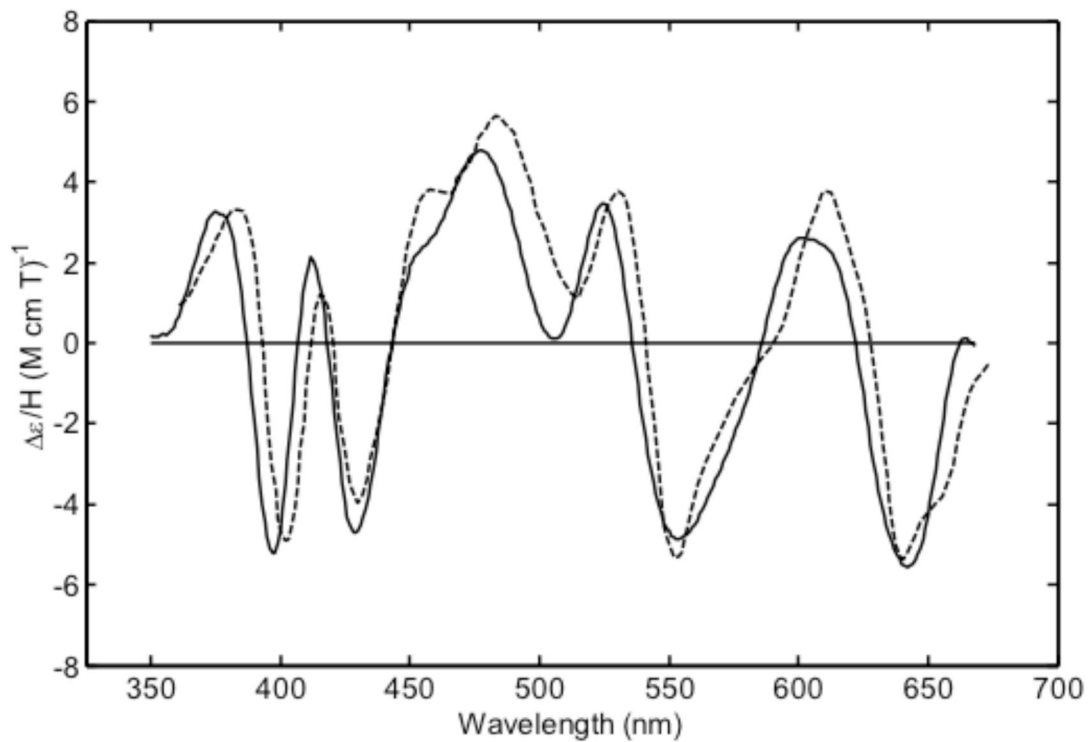


**Figure 5.** MCD spectra of ferric Dap1p in 25 mM HEPES buffer, pH 7.5, 22 °C (solid line) and ferric bovine liver catalase in 100 mM potassium phosphate buffer, pH 7.0, 14 °C (dashed line). The catalase spectrum was taken from the literature (47).